Fracture Properties of SPS Tungsten Copper Powder Composites

Medhat Awad El-Hadek & Saleh Hamada Kaytbay

Metallurgical and Materials Transactions A

ISSN 1073-5623
Volume 44
Number 1

Metall and Mat Trans A (2013)
44:544-551
DOI 10.1007/s11661-012-1396-x

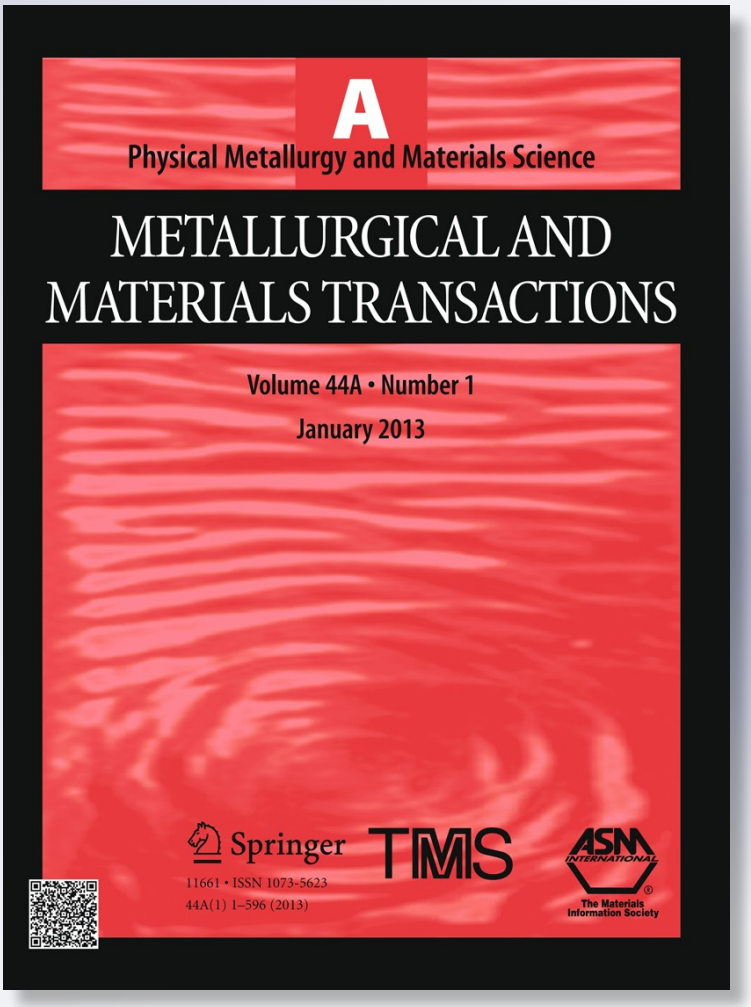

Springer

Fracture Properties of SPS Tungsten Copper Powder Composites

MEDHAT AWAD EL-HADEK and SALEH HAMADA KAYTBAY

Tungsten-copper composites with various copper nano-particles volume fractions were manufactured and examined. Tungsten-copper composites with 20 pct, 25 pct, and 30 pct volume fractions were mechanically mixed and sintered. spark plasma sintering (SPS) method was used for samples preparation at two different sintered temperatures 1273 K and 1373 K (1000 °C and 1100 °C). The effect of copper nano-particles on the bulk density, hardness, the coefficient of thermal expansion (CTE), electrical conductivity, and stress-strain behavior of the produced composites were studied. The hardness was found to decrease with the increase of the copper volume fraction in the composites. Conversely, the CTE and electrical conductivity increases with the increase of the copper volume fraction in the composites. Furthermore, the elastic modulus were extracted from tensile stress-strain behavior were found to increase with the increase of the copper volume fraction in the composites. Finally, the fracture surface roughness was studied using high resolution optical investigations and was noticeably higher with the increase of the copper volume fraction in the composites.

DOI: 10.1007/s11661-012-1396-x

I. INTRODUCTION

TUNGSTEN-COPPER (W-Cu) composites are characterized by high thermal conductivity, low thermal expansion and high wear resistance combined with excellent electrical conductivity.[1] The high thermal conductivity of copper and the low thermal expansion coefficient of tungsten make W-Cu composites attractive for thermal management materials in microelectronic devices.[2] Some of the potential applications can be summarized in electrical applications and high voltage arc contacts such as, electronic application includes, heat sinks and spreaders, microwave carriers, hermetic package bases, ceramic substrate carriers, and laser diode mounts.[3] Tungsten-copper composites are also reported to be used in wireless telecommunication devices as well as other power and radio-frequency packages for the microelectronics industry.[4,5] However, the W-Cu system exhibits mutual insolubility or negligible solubility.[6] W-Cu powder compacts show very poor sinterability, even by liquid phase sintering above the melting point of the Cu phase.[6]

The properties of composites depend strongly on the preparation method, particle size, and particle matrix interface adhesion. Particle size has a great role on the properties of the final composites. For example Bera *et al.*[7] have synthesized copper alloys with extended solid solubility and nano Al_2O_3 dispersion by mechanical alloying and equal channel angular pressing. It was found that the copper-Al_2O_3 alloys[7] appear to have high-strength, wear/erosion-resistant and Cu-based electrical contacts with nano-ceramic dispersion. Furthermore, Bera *et al.*[8] have developed a wear-resistant Cu-Cr-Ag electrical contacts alloy with nano-Al_2O_3 dispersion by mechanical alloying and high pressure sintering. It was reported[8] that the hardness and wear resistance of the Cu-Cr-Ag alloy with nano-Al_2O_3 dispersion increase significantly with the addition of nano-Al_2O_3 particles. El-Hadek, and Kaytbay[9] have reported that copper-Al_2O_3 composites with nano size Al_2O_3 particles have the lowest electrical resistivity values. This was attributed to the higher densification, generating a break in the continuous copper matrix network. As the Al_2O_3 particles sizes in the metal increases, the failure stresses decrease.[9] This leads to the reduction of the elastic modulus with the increase of Al_2O_3 particles sizes. Approximately 75 pct reduction in the elastic modulus between composites with Al_2O_3 particle size 100 nm, and 20 μm was evident.[9]

The classic conventional method for fabrication W-Cu composites is performed by the infiltration of a porous tungsten skeleton with liquid copper.[10] Infiltration is a two-step process that wicks molten copper into the open pores of a previously sintered tungsten porous structure. Since copper and tungsten are mutually insoluble, alloying does not occur in the general conditions (*i.e.*, pressures and temperatures) usually employed in the infiltration process. Following the infiltration stage, the parts are mechanically machined to the final dimensions. Moreover, the infiltration process does not result in a homogeneous microstructure and it is not a net shape process, thus causing high production costs.[10,11] In order to reduce cost and to produce net

MEDHAT AWAD EL-HADEK, Associate Professor, is with the Department of Mechanical Design & Production, Faculty of Engineering at Port-Said, Port-Said University, Port-Fouad, Port-Said 42523, Egypt. Contact e-mail: melhadek@eng.psu.edu.eg SALEH HAMADA KAYTBAY, Assistant Professor, is with the Department of Mechanical Engineering, Faculty of Engineering at Benha, Benha University, Benha, Egypt.

Manuscript submitted August 31, 2011.
Article published online September 19, 2012

shape components with homogeneous structure, high density W-Cu parts was produced by liquid-phase sintering of composite powders characterized by very fine dispersions of both metals.[12] The sinterability of W-Cu composites was increased by using SPS sintering process.[13] Lee *et al.*[14] has produced tungsten with 20 pct copper weight fraction composites with an average tungsten particle size of 1 μm. Lee *et al.*[14] have manufactured these composites without the addition of a sintering activator through a combination of the mechano-thermochemical process and liquid phase sintering.

Recently the spark plasma sintering (SPS) method of variation on field effect techniques has attracted considerable attention of researchers.[15–17] SPS method is simultaneous pulsed direct current used with uniaxial pressure to primarily sinter the powders. The SPS method used in sintering studies[16,17] is general related to the role of plasma that is generated between the powder particles.[18] While the concept of SPS plasma is rational, the role of the pulsed current remains not completely understood.[18] The main advantages of the SPS process is the fast heating rates reported to range from 323 K/min to 1273 K/min (50 °C/min to 1000 °C/min) and the uniform heating energy conditions.[19] In addition, the electrical current enhances the mass transport through electro-migration,[20] as well as the influence on the generation and mobility of point defects.[21]

The scope of this research is to manufacture tungsten-copper powder composites using SPS method with focused on characterizing tungsten-copper composite with various copper nano-particles volume fractions (20 pct, 25 pct, and 30 pct) at different sintering temperatures [1273 K and 1373 K (1000 °C and 1100°C)]. The powder composites were prepared by mechanically mixing two different volume fraction ratios according to the composition design and sintering by using SPS sintering. The microstructure surface was examined using high resolution optical analysis. The effect of copper nano-particles volume fraction on the bulk density, hardness, the coefficient of thermal expansion (CTE), electrical conductivity, and stress-strain behavior of the produced composites were investigated. Moreover, the fracture surface roughness was examined for all the tested composites.

II. MATERIALS PREPARATION

The importance of the SPS method as a tool for consolidating powders was the reason for selecting it as the method for preparing tungsten-copper (W-Cu) composites. The SPS process utilizes pulsed high current along with uniaxial pressure to consolidate powders through short time durations.[13] Two sintered temperatures were selected based on experimental observations namely 1273 K and 1373 K (1000 °C and 1100 °C). The melting temperature of copper the matrix material is 1357 K (1084 °C) as shown in Table I, so one of the sintered temperatures is above the melting temperature of copper to ensure encompassing of all the tungsten particles and the elimination of air gaps in the final composites.

Table I. Three Volume Fractions of Tungsten-Copper Composites

Volume Fraction	Tungsten Weight in Grams	Copper Weight in Grams
30 Pct Cu	83.4	16.6
25 Pct Cu	86.56	13.4
20 Pct Cu	89.6	10.4

When raising the temperature above 1373 K (1100 °C) the melted copper overfill the die and the bunch losses the volume fraction of the designed copper in the sample irregularly. This is due to the fact that the sintering process occurs during pressing. In case of lowering the sintering temperature below 1273 K (1000 °C) the copper in the samples does not completely melt and this leads to insufficient sintering. Purity of the tungsten used in SPS process for all composites was 99.85 pct and density was 19.3 g/cm^3, with an approximate particle size of 2 μm, and manufactured by H.C. Starck GmbH, Germany. The Young's Modulus for the tungsten used is 411 GPa, as body-centered cubic crystal structure, with apparent density of 3.6 g/cc, and tap density of 6.75 g/cc. Whereas, the copper powder used in all composites were electrolytic processed, with an approximate particle size of 35 μm and purity greater than 99 pct and density was 8.8 g/cm^3, manufactured by Alfa Aesar, USA. The Young's Modulus for the copper used ranges between 110 to 128 GPa, as face-centered cubic crystal structure, and with tap density of 3.8 g/cc.

To ensure uniformity of the particle shapes, the tungsten and the copper powders were mechanically milled and mixed in an agate rock mortar with high energy boll milled for half an hour with different volume ratios according to the composition design. The milling of the two powders resulted in uniform sphere-like nano-size particles for both tungsten and copper as presented in Figure 1(b). The powders were then loaded into a graphite die and were heated by passing an electric current through the assembly. SPS rapidly consolidate the composite powders to near theoretical density through the action of a rapid heating rate, pressure application, and proposed powder surface cleaning. The powder mixtures were spark plasma sintered at different temperatures at a heating rate of 200 °C/min under a pressure of 100 MPa in a vacuum atmosphere, using SPS-1050. This was generated by electrical discharge at the beginning of the pulsing. The direct current pulse energizing method generates the spark plasma, spark impact pressure, heating energy, as well as an electrical field diffusion effect.[13]

The tungsten and copper powders were weighted to form three different volume fraction composites calculated using Eq. [1]. The tungsten and copper densities are 19.3 and 8.96 g/cm^3, respectively.

$$V_f = \frac{\rho_m W_f}{\rho_m W_f + \rho_m W_f} \quad [1]$$

where V_f is the copper volume fraction, W_f is the weight of copper, W_m is the weight of Tungsten, ρ_f is the density of copper, and the ρ_m is the density of Tungsten. To ensure reputability of the composites, each powder was weighted separately and the three compositions of selections were made out of the weights presented in Table I.

The final densities of the materials were determined by the Archimedes method with deionized water as the immersion medium, as presented in Table II. The density of each sample was measured by taking its weight in air and in water. According to Archimedes role and MPIF standards, and ASTM- B328 standard,[22,23] the density ρ can be measured from Eq. [2]. Finally, melted wax of known density was used to coat the samples surface with a thin film of wax to isolate the surface porosity to prevent corrosion. The samples were weighted again in air.

$$\text{Density} = W_{air}/(W_{air} - W_{H_2O})\ \text{g/cm}^3 \qquad [2]$$

where W_{air} and W_{H_2O} are the weights in air and water respectively.

When comparing the tungsten-copper composites density to the tungsten theoretical density (19.3 g/cm^3) which forms the main structure of the composites, it is

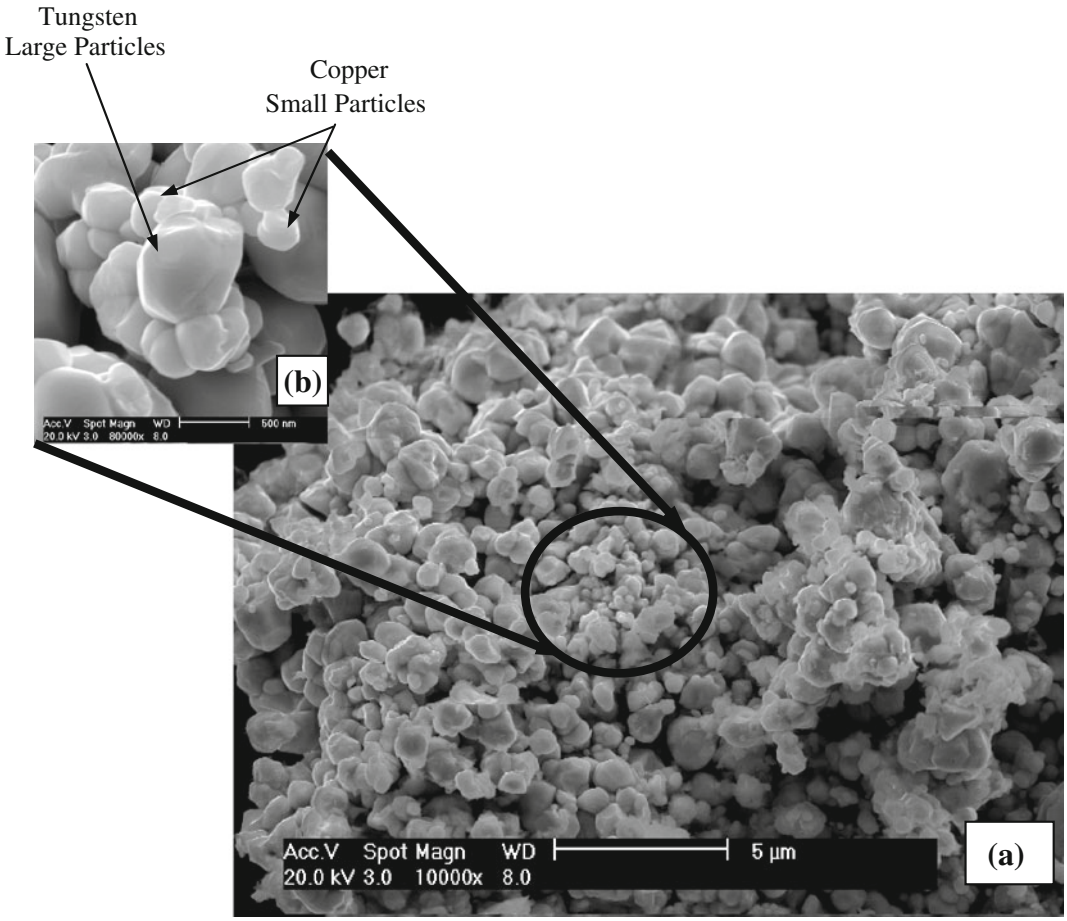

Fig. 1—(*a*) The surface microstructure of tungsten-copper composites with 30 pct copper volume fraction after using SPS, (*b*) magnification of the copper particles which are in the range of nano size that is relatively small compared to the tungsten particles.

Table II. The Three Densities of the Three Volume Fraction Tungsten-Copper Composites Under Two Sintered Temperatures Conditions Composites in Terms of g/cm^3, and in Terms of Pct to Tungsten Theoretical Density (19.3 g/cm^3)

	Density for Samples with 20 Pct Cu		Density for Samples with 25 Pct Cu		Density for Samples with 30 Pct Cu	
Sintering Temp. [K (°C)]	In Terms of g/cm^3	In Terms of Pct to *W* Density	In Terms of g/cm^3	In Terms of Pct to *W* Density	In Terms of g/cm^3	In Terms of Pct to *W* Density
1273 (1000)	15	77.7	14.6	75.6	13.8	71.5
1373 (1100)	14.3	74.1	14.8	76.7	13.9	72

clearly noticed that the with the increase of the copper volume fraction the relative density of the composite degreases. However, the density change of the investigated composites was not significant, other than tungsten-copper composites with 20 pct Cu where the density decreases with the increase of the sintering temperature. Moreover, it was also found that with the increase of the copper volume fraction in the composites the density decreases notably. This was explained through the HR-SEM images were the particle distribution was more homogeneous with increase of the copper volume fraction.

III. MATERIAL EXPERIMENTATION AND CHARACTERIZATION

A. *SEM Examinations*

The investigated copper-carbon composite materials were studied using scanning electron microscope (SEM) through the preparation process. High resolution scanning electron microscopy (HR-SEM) was performed with a Jeol 2000 FX analytical electron microscope operated at 200 kV to capture fine formations that SEM imaging cannot capture. A HR-SEM type FEI Tecnai F30 Super TWIN with a Schottky field emitter, using an acceleration voltage of 300 kV, point resolution limit 0.2 nm was used. The HR-SEM is equipped with a scanning transmission electron microscope (STEM) unit (smallest probe size 0.2 nm). For HR-SEM, the specimens were grinded, mechanically dimpled and thinned by Ar milling.

Figure 1 shows the surface microstructure of tungsten-copper composites with 30 pct copper volume fraction after using SPS. The upper left corner of Figure 1 presents a magnification of the copper particles which are in the nano size range that is relatively small compared to the tungsten particles. It was noticed the homogenous distribution of the copper particles (the small particles) through and surrounding the tungsten particles (the large particles). The high resolution scan imaging of the carbon powder particles was a challenging process, this was due to the light distraction associated with the particles morphology. It also could be explained due to the activation layer coating the tungsten powder particles, where the surface is shinier. The reason for this homogenous distribution could be explained by the HR-SEM images itself. Each tungsten particle was fully coated with nano copper precipitations allowing limited contact between the tungsten particles. This results in the reduction of the deboning zones throughout the materials. This homogenous distribution was reflected on the uniformity of the measured mechanical properties across the composites and the hardness across the composites thickness. It also improves the electrical conductivity of the composites.[2,10] So the SPS method was used on two different metals with nano sizes and the nano size is maintained in the final composites.

It should be observed that the particle sizes for the tungsten and copper have not significantly increased in size through the SPS, and after the sintering process because of the very short duration of the thermal exposure of the composites.

B. *Hardness Measurements*

Vickers microhardness, Hv, measurements were conducted using Neophot hardness tester and a load of (5 to 100 g) applied for 10 s. Vickers's microhardness measurements were carried out for the investigated composites of the two different sintering temperatures as well as for the three copper volume fraction composites using a load of 10 kg. To insure consistency though out the material surface and homogeneity, a minimum of ten readings were taken for each case which was of consistent as homogenous uniform distribution of the copper particles through and surrounding the tungsten particles observed through the SEM investigations. The Vickers micro-hardness results are presented in Table III.

It should be noticed that the specimens with the lowest copper volume fraction in the W-Cu composites were the hardest. As the increase of the copper volume fraction in the composites the hardness was found to decrease. The hardness values were notably increasing with the increase in sintering temperature. This is a reflection of the strong bonding between the particles for high sintering temperature, which is an indication of the high bulk density.

C. *Electrical Resistivity Measurements and Coefficient of Thermal Expansion*

The measured electrical resistivity was converted into the international annealed copper standard conductivity (IACS) units according to ASTM standards B193-72.[24] The electrical properties of copper were standardized in 1913 by the international electro technical commission which defined the IACS where the conductivity of copper was set at 100 pct. With its exceptional current carrying capacity, copper is more efficient than any other electrical conductor because of its superior conductivity. Annealed copper is the international standard which contains all other electrical conductors for comparison.[25] The electrical resistivity of the copper-carbon composites was measured by using high precision Micro-Ohmmeter, Omega CL8400. The electrical resistivity (ρ) was calculated according to Eq. [3]:

$$r = (R/A)L \qquad [3]$$

Table III. The Hardness (MPa) of the Three Volume Fraction in the Tungsten-Copper Composites Under Two Sintered Temperatures Conditions Composites

Sintering Temp. [K (°C)]	20 Pct Cu	25 Pct Cu	30 Pct Cu
1273 (1000)	1910	1880	1700
1373 (1100)	1920	1900	1720

Table IV. The Electrical Conductivity (pct IACS) of the Three Volume Fraction Tungsten-Copper Composites Under Two Sintered Temperatures Conditions Composites

Sintering Temp. [K (°C)]	20 Pct Cu	25 Pct Cu	30 Pct Cu
1273 (1000)	30	35	38
1373 (1100)	31	35	39

where R is the resistance in ohm, L is length (cm), A is the cross section (cm^2) and ρ is the electrical resistivity measured in $\mu\Omega$/cm.

Table IV presents the measured electrical conductivity in $\mu\Omega$/cm (which is $1/\rho$), for the W-Cu composites with three volume fractions of copper at two different sintering temperatures [1273 K and 1373 K (1000 °C and 1100 °C)]. The value of $(1/58 = 0.017241)$ mm^2 Ω/m is the international equivalent of volume resistivity of annealed copper equal to 100 pct electrical conductivity. The latter term means that a copper bar of 1 cm^2 in cross section at 293 K (20 °C) would have a resistance of 1.7241 $\mu\Omega$/cm.[24,25] All the measured resistivity data were converted to the international conductivity units (IACS) according to the latter relation. This was in contestant of the Chang *et al.*[26] observations, where the experimental resistivity of composites followed the trend of the theoretical prediction, increasing with increasing volume fraction. It was also noticed that the electrical conductivity (pct IACS) value changes with the sintering temperature were moderate, whereas the electrical conductivity (pct IACS) value increases with the increase of the sintered temperature.

It has been reported that there is a relation between the thermal conductivity and the electrical resistivity of a metal.[2,27] Heat transfer by conduction involves transfer of energy within a material without any motion of the material as a whole. The rate of heat transfer depends on the temperature gradient and the thermal conductivity of the material. Thermal conductivity is a reasonably straightforward concept. When you are discussing heat loss through the walls of your house, you can find tables which characterize the building materials and allow you to make reasonable calculations. More fundamental questions arise when you examine the reasons for wide variations in thermal conductivity. For metals, the thermal conductivity is quite high,[27] and those metals which are the best electrical conductors are also the best thermal conductors. At a given temperature, the thermal and electrical conductivities of metals are proportional, but raising the temperature increases the thermal conductivity while decreasing the electrical conductivity. Wiedemann and Franz[28] derived a relation equation between the thermal and electrical conductivities. Thus, if electrical resistivity can be measured, the thermal conductivity can be calculated this behavior is quantified in the Wiedemann-Franz Law as in the Eq. [4][28]:

$$\frac{\sigma\lambda}{T} = \frac{\pi^2 K_B^2}{3e^2} = L = 2.443 \times 10^{-8} \quad J\Omega/K^2s. \qquad [4]$$

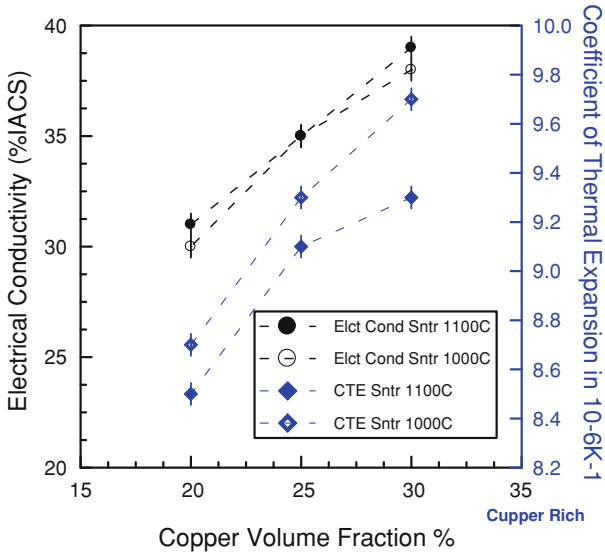

Fig. 2—The measured Electrical conductivity in (pct IACS), and the CTE in 10^{-6} K^{-1} for tungsten-copper composites with three volume fractions of copper and at two different sintering temperatures 1273 K and 1373 K (1000 °C and 1100 °C).

where λ is the thermal conductivity (W/mK), σ is the electric resistivity ($\mu\Omega$/cm), T is the ambient temperature [298 K (25 °C)], K_B is Boltzmann constant, and L is Lorentz number.

From the quantum mechanical point of view, the thermal conduction of the metal occurs by electron Fermi energy level. Thus the thermal conductivity can be expressed by the number of electrons and the effective mass of the electrons, which has Fermi energy level. Similarly, electrical conductivity can be expressed by the electrons. However, the electrical conductivity decreases with particle velocity increase because the collisions divert the electrons from forward transport of charge. This means that the ratio of thermal to electrical conductivity depends upon the average velocity squared, which is proportional to the kinetic energy. The proportional relationship between electrical conductivity and the CTE was observed and reported in Figure 2. The CTE was measured using a dilatometer of sensitivity of 10^{-4}. The CTE was measured in the temperature interval from 323 K to 523 K (50 °C to 250 °C). The linear CTE was calculated using the Eq. [5] as presented in Figure 2.

$$K = \Delta L/(L_0 \times \partial T) \qquad [5]$$

where K is linear CTE, ∂T is the temperature interval (change), ΔL is the relative length expansion due to temperature change as $\Delta L = (L - L_0)$, where L is the length of the sample after expansion, L_0 is the sample length before testing.

Since copper is one of the most important materials in electrical and electronic applications due to its high electrical conductivity.[2] Copper CTE is reported to be 17.6×10^{-6} K^{-1} [2] where the CTE of tungsten is 4.3×10^{-6} K^{-1}.[2] It could be noticed that the tungsten reinforced composites with the highest copper volume fraction have higher electrical conductivity. Further-

more, it is observed that the W-Cu composites with high volume fraction of copper have the highest CTE values, which could be attributed to the higher densification, generating a break in the continuous copper matrix network. Tungsten-copper composites are characterized by high thermal conductivity, high thermal expansion combined with excellent electrical conductivity.

D. *Tensile Mechanical Measurements*

Room temperature tensile experiments were conducted using MTS Testing Machine (Model 610) fitted with a 160 KN load cell operating in the displacement control mode. The electromechanical testing machine was conducted under quasi-static loading (strain rate of 8×10^{-5} to 1.3×10^{-4} s^{-1}). Cylindrical specimens with 5 mm in diameter and 20 mm in height were prepared from the cast rods. The contact surfaces of the samples were ground and polished to prevent frictional effects between the specimen and the punches. The samples were deformed until fracture occurred. To ensure consistency and homogeneity, a minimum of three samples for each case were subjected to the same loading conditions and the average value was reported in the results. The results indicated a measurement variation less than 8 pct. The stress-strain responses of the W-Cu composites with three volume fractions of copper and at one different sintering temperature 1273 K (1000 °C) were measured using the uniaxially tensile testing performed accordingly to ASTM standard E-9 for metals. The cross-head speed was 1 mm/min. The stress-strain responses were presented for three W-Cu composites with 20 pct, 25 pct, and 30 pct of copper volume fractions respectively, and at one sintering temperature of 1273 K (1000 °C) as shown in Figure 3.

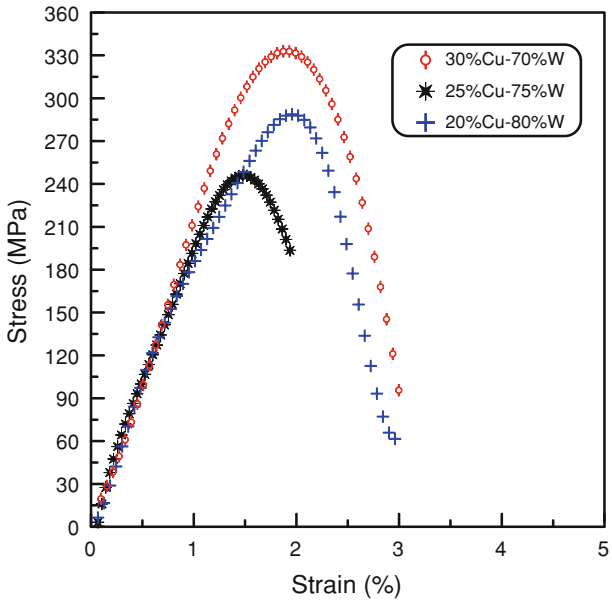

Fig. 3—The stress-strain responses for tungsten-copper composites with three volume fractions of copper and at 1273 K (1000 °C) sintering temperature.

For W-Cu composites with 30 pct volume fraction of copper, the stress-strain response was the highest, reflecting an elastic modulus value of 22071.51 MPa. As the copper volume fraction in the W-Cu composites decreases the failure strains decreases. This leads to the reduction of the elastic modulus, whose values decrease monotonically with the copper volume fraction over the entire range. The elastic modulus for W-Cu composites with 25 pct Cu was 19511.18 MPa, and for 20 pct Cu was 18021.18 MPa. Whereas, the failure strains for W-Cu composites with 30 pct, 25 pct, and 20 pct of Cu were 3.1 pct, 2.98 pct, and 1.94 pct, respectively. Also, by calculating the stiffness to weight ratio or specific stiffness, which is a materials property consisting of the elastic modulus per mass density of a material. The specific stiffness for W-Cu composites with 30 pct, 25 pct, and 20 pct volume fraction of copper were 16.38×10^6 $(m/s)^2$, 13.36×10^6 $(m/s)^2$ and 12.014×10^6 $(m/s)^2$, respectively. High specific stiffness materials find wide application in aerospace applications where minimum structural weight is required. For comparison purposes the specific stiffness for copper is reported to be 13×10^6 $(m/s)^2$, and for 21×10^6 $(m/s)^2$.[22,27] Approximately 18 pct reduction in the elastic modulus between composites with highest and the lowest copper volume fraction W-Cu composites is evident.

Close investigation of the fractured surfaces, as presented in Figure 4, shows a typical vein structure in the direction of the maximum shear stress. The direct observations of crystallization within the shear bands of W-Cu composites induced by bending are reported.[2,29] The fracture surface of the 30 pct volume fraction copper composite as shown in Figure 4(c) was found to have the roughest fracture surface as a reflection of the highest value of the ultimate tensile strength.

The top of the fractured specimens for the tungsten-copper composites is characterized by severe rough surface due to the release of the load at the final event of fracture in this very limited area, as presented in Figure 4 the higher magnification SEM. This could explain the high fracture strain that was noticed in Figure 3. The size of the nanocrystalline particles relative to the width of the nanocrystalline bands is critical in inducing the inhomogeneity in the flow deformation and micro-crack formation in the fracture composites.[30] The viscosity of the flow may have been increased with the help of the nanoscale particles, without forming any micro-cracks that leads to particle strengthening of the composites. Close investigation of the fractured surface specimen shows that the two layers (veins and featureless area) deform at different rates, since the vein-like layer is extruded out of the surface relative to the featureless layer, as shown in Figures 4(a) through (c).

IV. CONCLUSIONS

This research focuses on the manufacture of tungsten-copper composites using the SPS method with various copper nano-particles volume fractions (20 pct, 25 pct, and 30 pct) at different sintering temperatures [1273 K

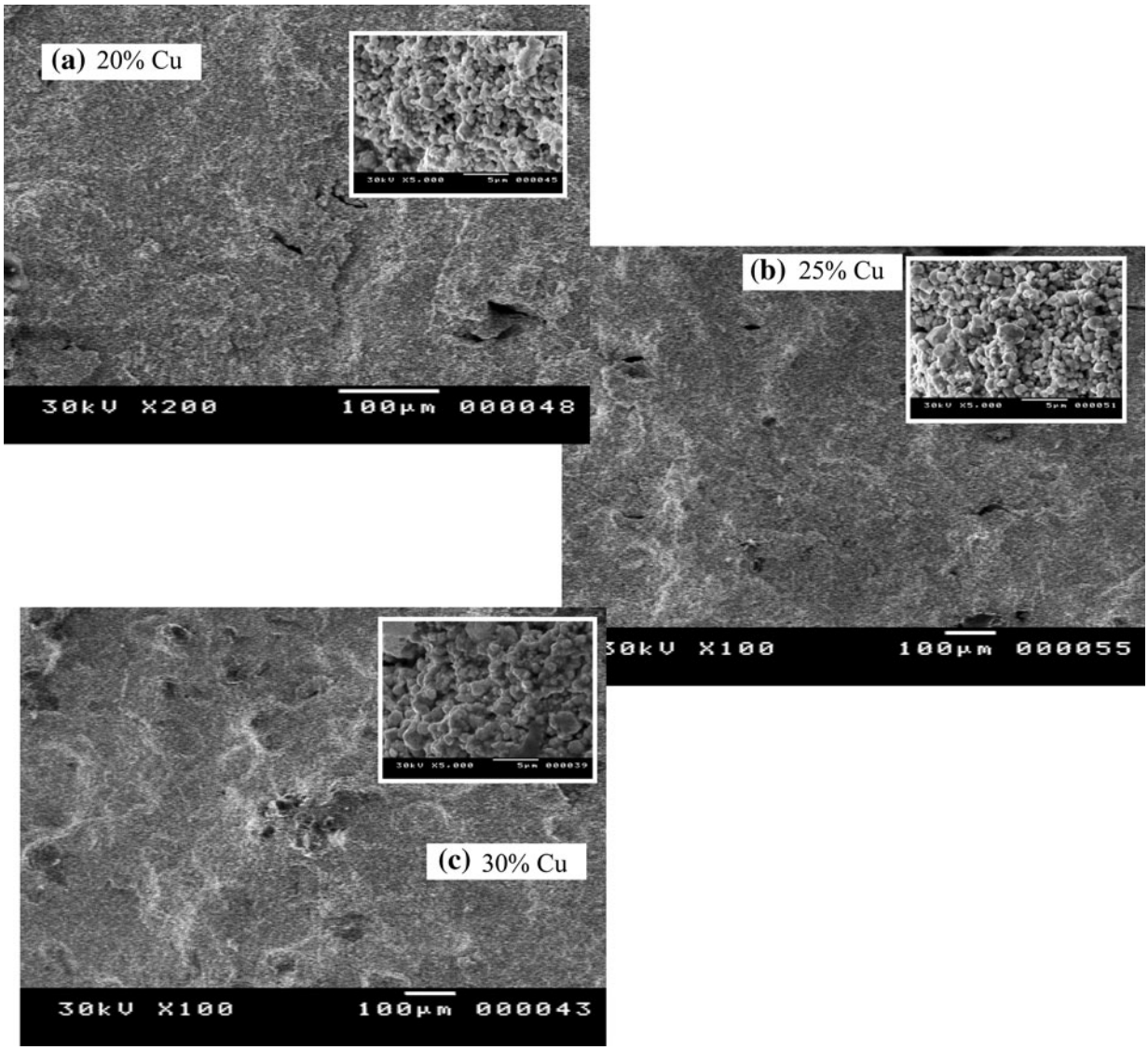

Fig. 4—The SEM fracture surfaces and higher magnifications at the top the fractured tungsten-copper composites for copper volume fractions of (*a*) 20 pct, (*b*) 25 pct, and (*c*) 30 pct, at 1273 K (1000 °C) sintering temperature.

and 1373 K (1000 °C and 1100 °C)]. Evaluation and determination of the effect of different copper volume fraction and sintering temperature on the mechanical, electrical, and fracture properties of the composites were successfully achieved. HR-SEM investigations revealed homogenous distribution of the copper particles surrounding the tungsten particles. The hardness of the composites was found to monotonically decreasing with the increase of the copper volume fraction in the composites and increase with the increase of the sintering temperature. This was a reflection of the strong bonding between the particles at high sintering temperatures, which indicates high bulk density. Similarly the Electrical conductivity (pct IACS) increases with increase of the copper volume fraction in the composites and increase with the increase of the sintering temperature.

For the tungsten-copper composites with higher volume fraction of copper, the stress-strain response was the highest. The stress-strain response decreases with the decrease of copper volume fraction in the W-Cu composites. This is due to the nanostructure of the composites with high volume fraction of copper and the inter-granular surface that contributes in affecting the stress-strain of the composites. This explains the fact that the composites with high volume fraction of copper show high fracture strain values compared to the composites with lower volume fraction of copper. Furthermore, it clarifies why the crack faces higher resistance in penetrating through composites at higher copper volume fraction than composites with lower copper volume fraction. Approximately 30 pct reduction in the elastic modulus between W-Cu composites of 30 pct, and 20 pct copper volume fraction respectively.

Conversely, the specific stiffness increases with the increase of the copper volume fraction in the composites which reflects good bonding between two different types of elemental powders that have no solubility.

REFERENCES

1. J.L. Johnson and R.M. German: *J. Adv. Powder Metall.*, 1991, vol. 6, pp. 391–405.
2. Y.D. Kim, N.L. Oh, S.T. Oh, and I.H. Moon: *Mater. Lett.*, 2001, vol. 51 (5), pp. 420–24. doi:10.1016/S0167-577X(01)00330-5.
3. E. Uhlmann, S. Piltz, and K. Schauer: *J. Mater. Process. Technol.*, 2005, vol. 167, pp. 402–07. doi:10.1016/j.jmatprotec.2005.05.022.
4. E.S. Yoon, J.S. Lee, S.T. Oh, and B.K. Kim: *Int. J. Refract Metal Hard Mater.*, 2002, vol. 20 (3), pp. 201–06. doi:10.1016/S0263-4368(02)00003-3.
5. S.H. Hong and B.K. Kim: *Mater. Lett.*, 2003, vol. 57 (18), pp. 2761–67. doi:10.1016/S0167-577X(03)00071-5.
6. F. Doré, S. Lay, N. Eustathopoulos, and C.H. Allibert: *Scripta Mater.*, 2003, vol. 49 (3), pp. 237–42. doi:10.1016/S1359-6462(03)00244-6.
7. S. Bera, Z. Zúberová, R.J. Hellmig, Y. Estrin, and I. Manna: *Philos. Mag.*, 2010, vol. 90 (11), pp. 1465–83. doi:10.1080/14786430903365286.
8. S. Bera, W. Lojkowsky, and I. Manna: *Metall. Mater. Trans. A*, 2009, vol. 40A, pp. 3276–83. doi:10.1007/s11661-009-0019-7.
9. M.A. El-Hadek and S. Kaytbay: *Strain*, 2009, vol. 45 (6), pp. 506–15. doi:10.1111/j.1475-1305.2008.00552.x.
10. J. Cheng, P. Song, Y. Gong, Y. Cai, and Y. Xia: *Mater. Sci. Eng.*, 2008, vol. 488, pp. 453–57. doi:10.1016/j.msea.2007.11.022.
11. A.K. Basu and F.R. Sale: *J. Mater. Sci.*, 1978, vol. 13, pp. 2703–11.
12. M.B. Naseri, A.R. Kamali, and S.M. Hadavi: *Russ. J. Inorg. Chem.*, 2010, vol. 55 (2), pp. 167–73. doi:10.1134/S0036023610020051.
13. Z.A. Munir, U. Anselmi-Tamburini, and M. Ohyanagi: *J. Mater. Sci.*, 2006, vol. 41, pp. 763–77. doi:10.1007/s10853-006-6555-2.
14. G.G. Lee, G.H. Ha, and B.K. Kim: *Powder Metall.*, 2000, vol. 43 (1), pp. 79–82.
15. M. Omori: *Mater. Sci. Eng. A*, 2000, vol. 287 (2), pp. 183–88. doi:10.1016/S0921-5093(00)00773-5.
16. J.R. Groza: *Powder Metall. Met. Handb.*, 1998, vol. 7, pp. 583–89.
17. J.R. Groza, M. Garcia, and J.A. Schneider: *J. Mater. Res.*, 2001, vol. 16, pp. 286–92. doi:10.1557/JMR.2001.0043.
18. M. Tokita: *Mater. Sci. Forum*, 1999, vols. 308–311, pp. 83–88. doi:10.4028/www.scientific.net/MSF.308-311.83.
19. U. Anselmi-Tamburini, J.E. Garay, and Z.A. Munir: *Mater. Sci. Eng. A*, 2005, vol. 407, pp. 24–30. doi:10.1016/j.msea.2005.06.066.
20. T.B. Holland, J.F. Loffler, and Z.A. Munira: *J. Appl. Phys.*, 2004, vol. 95 (5), pp. 2896–99. doi:10.1063/1.1642280.
21. P. Asoka-Kumar, K. O'Brien, K.G. Lynn, P.J. Simpson, and K.P. Rodbell: *Appl. Phys. Lett.*, 1996, vol. 68, pp. 406–08. doi:10.1063/1.116700.
22. M.H. Maneshian and A. Simchi: *J. Compos. Compd.*, 2008, vol. 463, pp. 153–59. doi:10.1016/j.jallcom.2007.08.080.
23. Keithely: *Low-Level Measurements Handbook*. Anablog-Blog on EDN, New York Publications, 1991.
24. IACS: Electrical properties. International Annealed Copper Standard by the International Electro Technical Commission (IACS) in terms of the following properties at 20 °C, 1913.
25. G. Weng: *Int. J. Eng. Sci.*, 1984, vol. 22 (7), pp. 845–56. doi:10.1016/0020-7225(84)90033-8.
26. S.-Y. Chang, C.-F. Chen, S.-J. Lin, and T.Z. Kattamis: *Acta Mater.*, 2003, vol. 51 (20), pp. 6291–302. doi:10.1016/S1359-6454(03)00462-2.
27. D. Janković Ilić, J. Fiscina, C.J.R. González-Oliver, N. Ilić, and F. Mücklich: *J. Mater. Sci.*, 2008, vol. 43 (20), pp. 6777–83. doi:10.1007/s10853-008-2941-2.
28. S. Raymond: *Physics for Scientists and Engineers with Modern Physics*, 3rd ed., Saunders College Publishing, Forth Worth.
29. A. Abousree Hegazy, M. Abdallah, A. Ibrahim, and S.F. Mostafa: *Res. Bull. Aust. Inst. High Energ. Mater.* This manuscript has been reviewed and accepted for publication in the 2010, ISBN: 978-0-9806811-8-5, http://bulletins.ausihem.org/.
30. X. Shi, S. Wang, X. Yang, Q. Zhang, and Y. Wang: *J. Wuhan Univ. Technol. (Mater. Sci. Ed.)*, 2010, vol. 25 (6), pp. 909–13. doi:10.1007/s11595-010-0118-8.